

# Relations between X-ray timing features and spectral parameters of Galactic black hole X-ray binaries

H. Stiele<sup>1\*</sup>, T. M. Belloni<sup>1</sup>, E. Kalemci<sup>2</sup>, and S. Motta<sup>3</sup>

<sup>1</sup>*INAF-Osservatorio Astronomico di Brera, Via E. Bianchi 46, I-23807 Merate (LC), Italy*

<sup>2</sup>*Sabancı Üniversitesi, Orhanlı-Tuzla, 34956 Istanbul, Turkey*

<sup>3</sup>*European Space Astronomy Centre (ESAC)/ESA, PO Box 78, E-28691 Villanueva de la Cañada, Madrid, Spain*

2012 December 3

## ABSTRACT

We present a study of correlations between spectral and timing parameters for a sample of black hole X-ray binary candidates. Data are taken from GX 339-4, H 1743-322, and XTE J1650-500, as the *Rossi X-ray Timing Explorer* (RXTE) observed complete outbursts of these sources. In our study we investigate outbursts that happened before the end of 2009 to make use of the high-energy coverage of the HEXTE detector and select observations that show a certain type of quasi-periodic oscillations (type-C QPOs). The spectral parameters are derived using the empirical convolution model `simpl` to model the Comptonized component of the emission together with a disc blackbody for the emission of the accretion disc. Additional spectral features, namely a reflection component, a high-energy cut-off, and excess emission at 6.4 keV, are taken into account. Our investigations confirm the known positive correlation between photon index and centroid frequency of the QPOs and reveal an anti-correlation between the fraction of up-scattered photons and the QPO frequency. We show that both correlations behave as expected in the “sombbrero” geometry. Furthermore, we find that during outburst decay the correlation between photon index and QPO frequency follow a general track, independent of individual outbursts.

**Key words:** X-rays: binaries – X-rays: individual: GX 339-4, H 1743-322, XTE J1650-500 – binaries: close – black hole physics

## 1 INTRODUCTION

Most known black hole X-ray binaries (BHT) are transient. They are only observable during outbursts, as they are too faint to be detectable with present X-ray instruments during quiescence (see e.g. Garcia et al. 1998). While a BHT is in outburst it evolves through different states, which show characteristic timing and spectral properties. The states can be identified with the help of the hardness intensity diagram (HID; Homan et al. 2001; Belloni et al. 2005; Homan & Belloni 2005; Gierliński & Newton 2006; McClintock & Remillard 2006; Fender et al. 2009; Belloni et al. 2011), the hardness-rms diagram (HRD; Belloni et al. 2005), and the rms-intensity diagram (RID; Muñoz-Darias et al. 2011). In general, outbursts begin and end in the low hard state (LHS) and there is a transition to the high soft state (HSS) in between. Three different types of low frequency quasi-periodic oscillations (LFQPOs) can be distinguished in BHTs (Casella et al. 2005; Wijnands et al. 1999). In the LHS and the hard intermediate state (HIMS; following the nomenclature of Belloni 2010) a specific timing feature named type-C QPOs can be observed (Belloni et al. 2011).

Existence of a correlation between the QPO frequency and the photon index was first shown by Di Matteo & Psaltis (1999). They focused their discussion on the implications of the limited QPO frequency band on the limited change in the inner disc radius during transitions. Shaposhnikov & Titarchuk (2009) studied correlations between the centroid frequency of QPOs and spectral parameters for a sample of eight BHTs observed with the Rossi X-ray Timing Explorer (RXTE). To obtain the spectral parameters RXTE/PCA (Proportional Counter Array) spectra in the 3.0 – 50.0 keV range were fitted with the `bmc` model (Titarchuk et al. 1997), which is hardwired to a Planck function.

In this paper we investigate correlations between spectral parameters and timing properties for a sample of seven outbursts from three different sources. The spectra are fitted with a disk blackbody convolved with the `simpl` model (Steiner et al. 2009), which is an empirical model of Comptonization. To model the broad spectral features due to reflection accurately, and to determine a high-energy cut off – if present –, we included RXTE/HEXTE data in our study. We used only observations that showed type-C QPOs. A discussion of the correlation between photon index and centroid frequency for type-B QPOs observed in the 2010 outburst of GX 339-4 can be found in Stiele et al. (2011).

\* E-mail: holger.stiele@brera.inaf.it

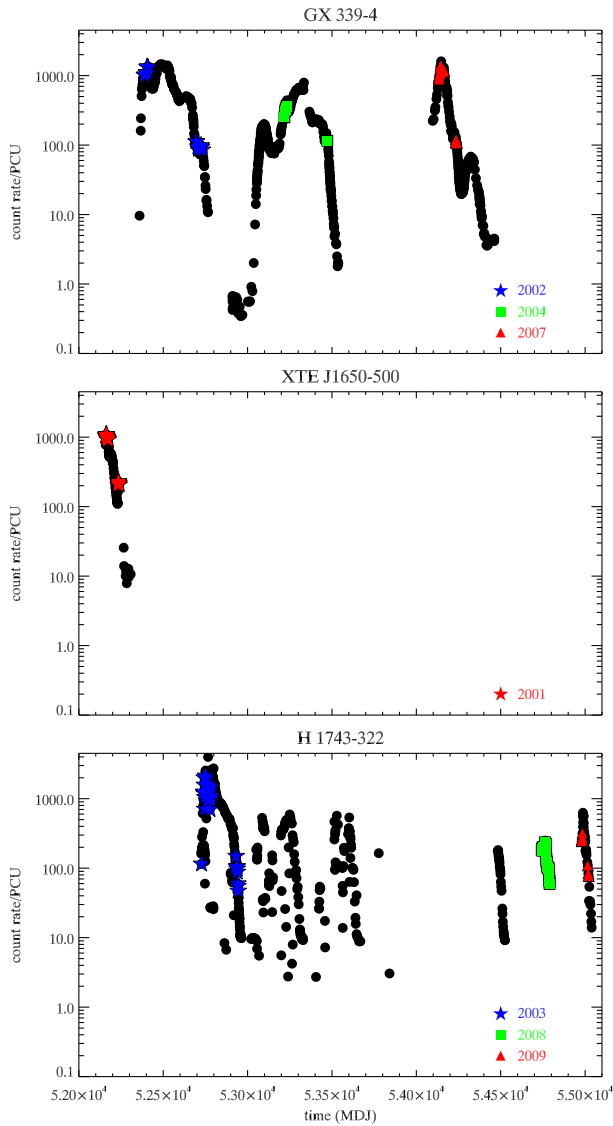


**Figure 1.** Long-term PCA light curves of GX 339-4 (upper panel), XTE J1650-500 (middle panel), and H 1743-322 (lower panel). Each point corresponds to an entire observation. The observations used in our study are marked with different symbols.

## 2 OBSERVATIONS AND DATA ANALYSIS

In this paper we analysed archival RXTE observations of several outbursts of the black hole X-ray binary candidates GX 339-4, H 1743-322, and XTE J1650-500, namely:

- the 2002/03, 2004, and 2007 outbursts of GX 339-4
- the 2003, 2008, and 2009 outbursts of H 1743-322
- and the 2001 outburst of XTE J1650-500, which is the only observed outburst of this source.

We selected these sources as RXTE observed complete outbursts of them, i. e. neither the initial rise nor the decay to quiescence is missing; a substantial number of observations with type-C QPOs have been detected; and the HIDs were nicely q-shaped. In addition, RXTE observed several outbursts of GX 339-4 and H 1743-322, including outbursts at different luminosities and one outburst of H 1743-322 that did not go all the way to the soft state

(Motta et al. 2010, 2011). Long-term PCA light curves are given in Fig. 1. Outbursts that happened either partially or totally after the end of 2009 have been excluded from our study to avoid the introduction of systematic uncertainties in the spectral parameters due to the strong residuals in the HEXTE spectra that are related to the difficulties in determining the background contribution since technical problems occurred in the HEXTE detector (see also Stiele et al. 2012). We investigated the timing and spectral properties, as described below.

### 2.1 Timing analysis

The values of the centroid frequencies and the classification of the QPOs for all three outbursts of GX 339-4 have been published in Motta et al. (2011), and for the 2008 and 2009 outbursts of H 1743-322 in Motta et al. (2010). The data of the 2001 outburst of XTE J1650-500 were analysed using the methods and classification criteria described in these papers. We used data from the Proportional Counter Array (PCA) to compute power density spectra (PDS) for each observation following the procedure outlined in Belloni et al. (2006). PDS production has been limited to the PCA channel band 0 – 35 (2 – 15 keV) and used 16 second long stretches of Event mode data. For observations which showed a quasi-periodic oscillation (QPO) we subtracted the contribution due to Poissonian noise (Zhang et al. 1995), normalised the PDS according to Leahy et al. (1983) and converted it to square fractional rms (Belloni & Hasinger 1990). We determined the centroid QPO frequency, by fitting the noise components as well as the QPO feature with Lorentzians, following Belloni et al. (2002). PDS fitting was carried out within the standard `xspec` fitting package (Arnaud 1996) by using a one-to-one energy–frequency conversion and a unit response. The observations of XTE J1650-500 during outburst decay have been already analysed in Kalemci et al. (2003). They used a 2 – 30 keV energy range with 128 second long stretches<sup>1</sup>. For the 2003 outburst of H 1743-322 we took the QPO frequencies listed in Table 2A of McClintock et al. (2009). They used the full bandwidth of the PCA instrument (2 – 40 keV) and searched for QPOs in the 4 mHz to 4 kHz range with a sliding frequency window technique (Remillard et al. 2002a,b). In the following, we focus on observations which QPOs we have classified as type-C.

### 2.2 Spectral analysis

For all observations with type-C QPOs we used the PCA Standard 2 mode (STD2), which covers the 2–60 keV energy range with 129 channels, and the HEXTE Standard mode, which covers the 15–250 keV energy range with 129 channels, for the spectral analysis. The standard RXTE software within `HEASOFT V. 6.9` was used to extract background and dead-time corrected energy spectra for each observation. Solely Proportional Counter Unit 2 from the PCA was used since only this unit was on during all the observations. To account for residual uncertainties in the instrument calibration a systematic error of 0.6 per cent was added to the PCA spectra<sup>2</sup>. For observations taken between 2001 and 2004 we used HEXTE data

<sup>1</sup> Using 16 second long or 128 second long stretches does not lead to any change in the derived QPO centroid frequency, as type-C QPOs are strong, narrow features in the PDS.

<sup>2</sup> A detailed discussion on PCA calibration issues can be found at: <http://www.universe.nasa.gov/xrays/programs/rxte/pca/doc/rmf/pcarmf-11.7/>

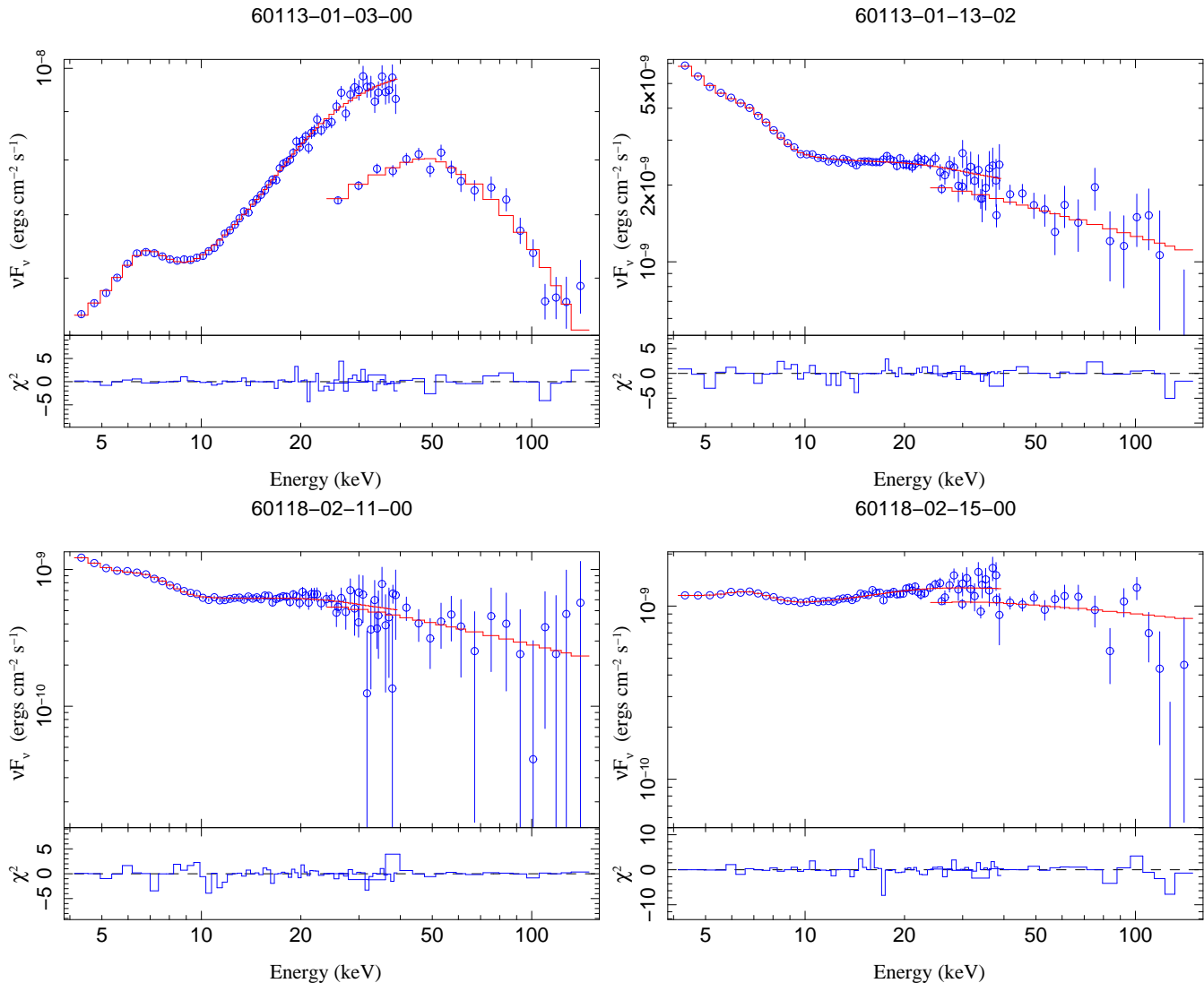


**Figure 2.** Unfolded spectra of XTE J1650-500 at the begin (upper left) and end (upper right) of the rise and at the begin (lower left) and end (lower right) of the decay of its outburst.

from cluster A, while for observations taken in 2007, 2008, and 2009 cluster B data have been used.

Combined PCA+HEXTE spectra were fitted within *ISIS* V. 1.6.1 (Houck & Denicola 2000) in the 4 – 40 keV and 22 – 200 keV range. We uniformly fitted the spectra with a partially Comptonized multi-color disc blackbody model, including foreground absorption. Four  $\nu F_\nu$  spectra of XTE J1650-500 taken from the beginning and end of the rise and decay branch, respectively, are shown as examples in Fig. 2. *ISIS* “unfolded spectra” are independent of the assumed spectral model (i.e., the unfolding is done solely with the response matrix and effective area files; see Nowak et al. 2005 for details). The plotted residuals, however, are those obtained from a proper forward-folded fit. The disc emission was approximated by the *diskbb* model (Mitsuda et al. 1984) and the *simpl* model (Steiner et al. 2009) was used for Compton scattering. The latter one being an empirical convolution model that converts a given fraction of the incident spectrum into a power law shape with a photon index  $\Gamma$ . The amount of the up-scattered fraction of the incident radiation is stored in a parameter called scattered fraction. We allowed for a reflection component and mod-

eled it with *reflect* (Magdziarz & Zdziarski 1995). The reflection component affected solely the up-scattered photons (see also Gou et al. 2011; Tamura et al. 2012). As *simpl* and *reflect* are convolution models it is necessary to calculate the model well outside the normal bounds of the PCA and HEXTE energy range. Therefore, we used an extended energy range from 0.1 keV to 1 MeV for our fits. The distribution of reflection values for all three sources are shown in Fig. 3. The mean error is about 0.15 (GX 339-4, XTE J1650-500) to 0.2 (H 1743-322), although individual observations can show much smaller or bigger errors. If needed a high-energy cut-off (*highcut*) was included. This was mostly the case for observations observed during the rise of an outburst. We added a Gaussian to account for excess emission at 6.4 keV. The centroid was allowed to vary between 6.4 and 6.7 keV and the line width was constrained between 0 and 1 keV to prevent artificial broadening due to the response of the PCA detector at 6.4 keV. For the foreground absorption we used the *TBabs* model (Wilms et al. 2000), with fixed foreground absorption ( $N_H$ ). Values used for the individual sources are:  $5.0 \times 10^{21} \text{ cm}^{-2}$  for GX 339-4 (Zdziarski et al. 2004),  $1.6 \times 10^{22} \text{ cm}^{-2}$  for H 1743-322 (Capitanio et al. 2009), and

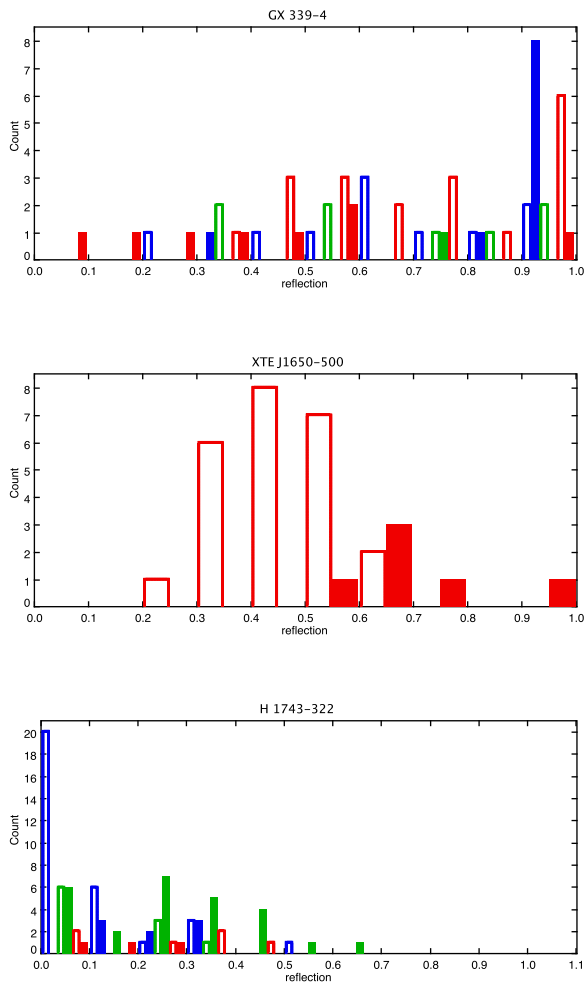


**Figure 3.** Distribution of the reflection values for GX 339-4 (upper panel), XTE J1650-500 (middle panel), and H 1743-322 (lower panel) with a binning of 0.1. The mean error is about 0.15 (GX 339-4, XTE J1650-500) to 0.2 (H 1743-322). Open bars denote observations belonging to the rise branch of an outburst, while filled bars mark observations of the decay branch. Different outbursts are marked with different colours (grey shades), using the same colouring scheme as in Figs. 1 and 4.

$6.7 \times 10^{21} \text{ cm}^{-2}$  for XTE J1650-500 (Tomsick et al. 2004). For most observations the disc blackbody temperature lies between 0.5 and 1.2 keV and we obtain an inner disc radius of a few tens kilometers. The reduced  $\chi^2$  value,  $\chi_{\text{red}}^2 = \chi^2/N_{\text{dof}}$ , where  $N_{\text{dof}}$  is the number of degrees of freedom (dof), is less than or around one for most of the observations. For a small fraction ( $\approx 2\%$ ) of spectra the value of  $\chi_{\text{red}}^2$  exceeds 1.5. However, it never reaches a rejection limit of two.

### 3 CORRELATIONS

In this section we present correlations between QPO centroid frequency and different spectral parameters. Figure 4 shows for the three BHTs the correlations between QPO centroid frequency and photon index or scattered fraction, respectively. Individual outbursts of the same source are marked with different symbols. The broad distribution of reflection fractions (see Fig. 3) and the rather large systematic errors hamper the detection of any clear trends

in the correlation between reflection fraction and QPO frequency. We do not show correlations between QPO frequencies and disc parameters, as the obtained disc parameters should be taken with care. The working range of PCA (3 – 40 keV) covers only the high energy part of the disc component, above the Wien peak. The missing coverage of lower energies together with the presence of a strong Comptonized component increases the uncertainties in the derived disc parameters, especially for observations obtained at the very begin and end of an outburst. In addition, it is known that the spectral parameters derived from the `diskbb` model should not be interpreted literally (see e.g. Merloni et al. 2000; Remillard & McClintock 2006). Nevertheless, we want to mention that our investigations imply that QPOs at the same frequency occur at a lower inner disc radius in the decay branch compared to the rise branch.

#### 3.1 The scattered fraction – QPO centroid frequency relation (SF-QPO relation)

All investigated outbursts show a negative correlation between the fraction of up-scattered photons and the QPO centroid frequency: a high scattered fraction is observed at low QPO frequencies, and the scattered fraction decreases with increasing frequency. In the case of XTE J1650-500 the correlation is most obvious and we recognise two branches which belong to the rise and decay branch of the outburst, where the latter one lies above the branch of the rise. For the other two sources the distinction between rise and decay is less clear. For H 1743-322 it is impossible to separate different branches. For a few observations we obtained a scattered fraction close to unity. In these cases we used the  $1\sigma$  lower error as a lower limit (indicated in Fig. 4 by a small arrow).

#### 3.2 The photon index – QPO centroid frequency relation ( $\Gamma$ -QPO relation)

The photon index rises with increasing QPO centroid frequency. In the case of XTE J1650-500 it is a shallow and rather linear rise. The two branches belonging to the rise and decay of the outburst are indistinguishable. We recognise distinct rise and decay branches for the 2002 and 2007 outburst of GX 339-4. The branch belonging to the rise of the 2004 outburst seems to be aligned with the decay branch of the 2002 outburst. This might be related to the lower luminosity at which the 2004 outburst has been observed. The photon indices are well constrained. The  $\Gamma$ -QPO relation in GX 339-4 can be described as a loop-like structure compared to the narrower, more band-like appearance in the case of H 1743-322.

#### 3.3 $\Gamma$ -QPO relation during outburst decay

In Fig. 5 (left column) we summarised in one diagram the  $\Gamma$ -QPO relation during decay for all outbursts. This figure reveals that the  $\Gamma$ -QPO relation follows a general track during outburst decay. The relation can be approximated by  $\Gamma = \Gamma_0 + a * cf_{\text{QPO}}$ , with  $\Gamma_0 = 1.73$  and  $a = 0.08$ . The standard deviation in  $\Gamma$  is 0.10. We would like to point out that during outburst decay also the distribution of source luminosities is narrower.

#### 3.4 SF-QPO relation during outburst decay

In Fig. 5 (right column) we summarised in one diagram the SF-QPO relation during decay for all outbursts. Unlike the  $\Gamma$ -QPO rela-

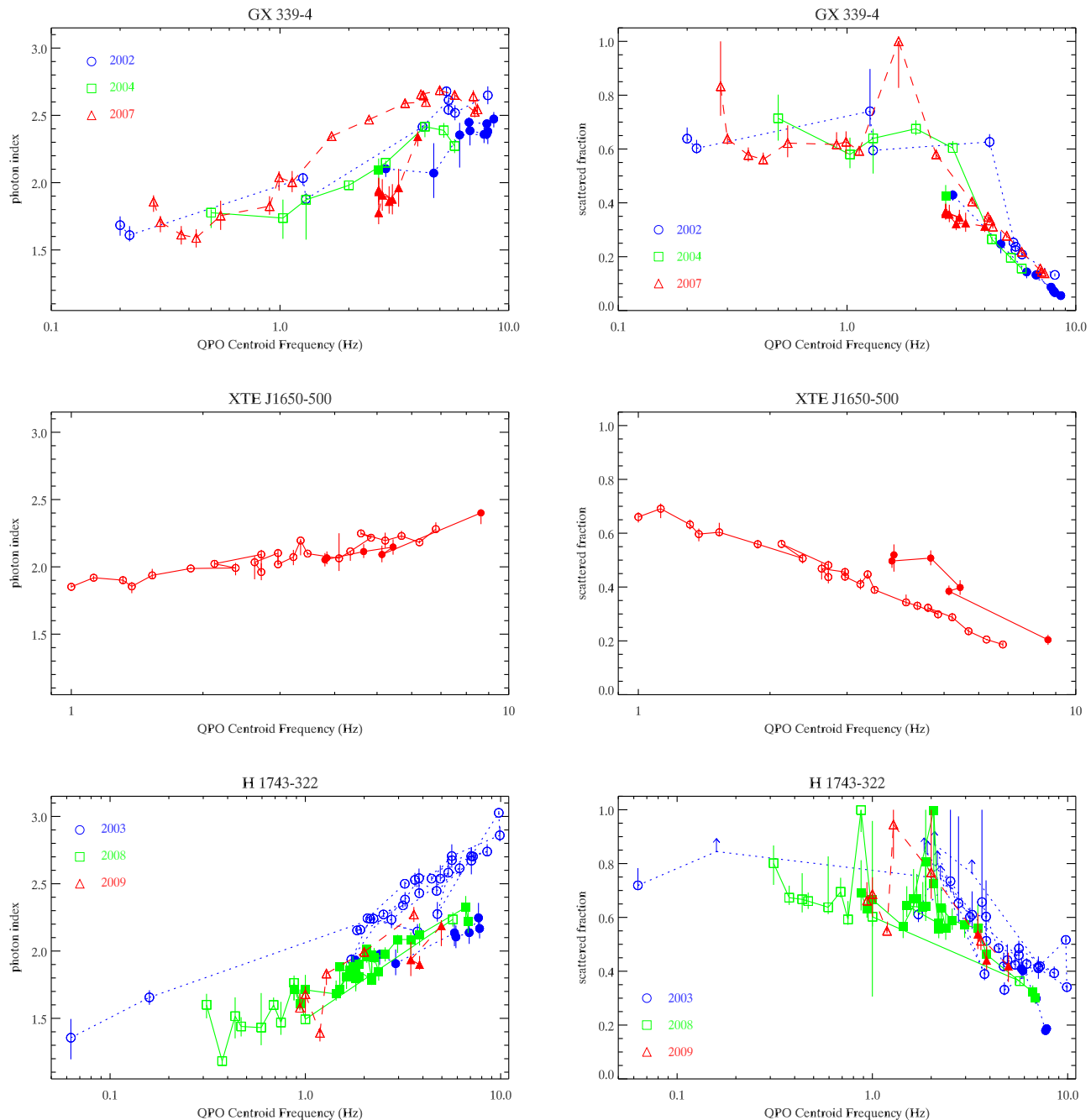


**Figure 4.**  $\Gamma$ -QPO (left column) and SF-QPO (right column) correlations for GX 339-4 (upper row), XTE J1650-500 (middle row), and H 1743-322 (lower row). Open symbols denote observations belonging to the rise branch of an outburst, while filled symbols mark observations of the decay branch. If a source has been detected during more than one outburst, the individual outbursts are marked with different symbols. Observations for which we obtained only a lower limit of the scattered fraction are marked by arrows.

tion, the SF-QPO relation shows two tracks. The upper one consists of all observations of XTE J1650-500 and of most observations of H 1743-322. The lower track contains the observations of GX 339-4. Only, the 2003 outburst of H 1743-322 starts at  $\sim 7$  Hz on the correlation of GX 339-4, leaves it and reaches the upper track spanned by the other observations of H 1743-322.

#### 4 DISCUSSION

We studied for the BHTs GX 339-4, H 1743-322, and XTE J1650-500 the correlation between the QPO centroid frequency and two spectral parameters: the photon index and the fraction of up-scattered photons. The correlations presented in this work agree qualitatively with the ones that can be derived from the values given in Table 2 of Shaposhnikov & Titarchuk (2009). This means that the anti-correlation in the SF-QPO relation and the positive correla-



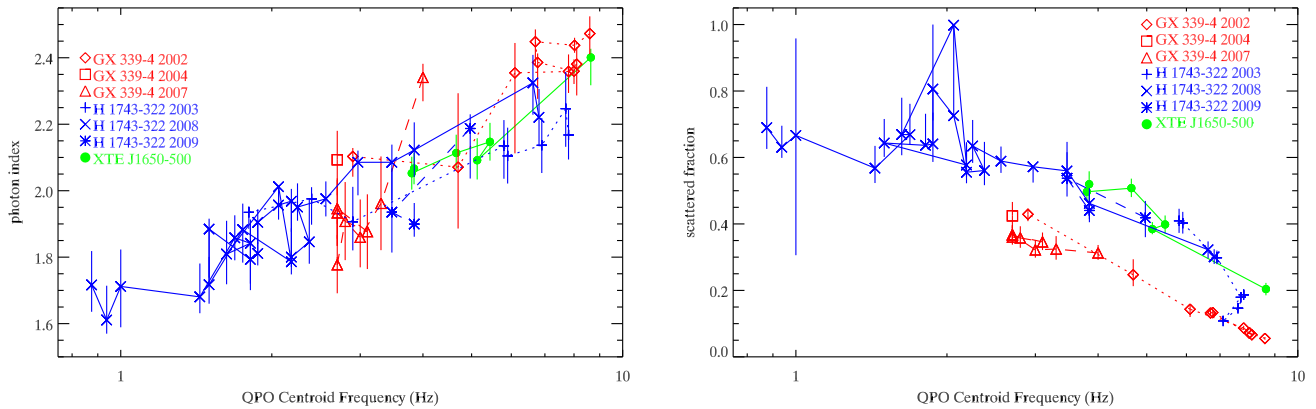


**Figure 5.** The  $\Gamma$ -QPO (left column) and SF-QPO (right column) relation during decay for all seven outbursts. In the  $\Gamma$ -QPO diagram all points seem to follow the same track, without recognisable differences between individual sources. In the SF-QPO diagram there are two different tracks. The points obtained from observations of H 1743-322 and XTE J1650-500 are located on one track, while those of GX 339-4 span their own track at lower scattered fractions.

tion in the  $\Gamma$ -QPO relation are model independent. We note that the photon indices in the present work are slightly higher than those derived with the *bmc* model. This has to be expected, as we included a reflection component in our spectral model. Vignarca et al. (2003) investigated the correlation between QPO frequency and photon index for an additional five sources, partially taking QPO frequencies and spectral parameters from the literature. A single correlation between spectral index and QPO centroid frequencies was also found by Kalemci (2002) during the outburst decays of six sources in eight outbursts.

X-ray spectra of black hole X-ray binaries consist of two main components: The soft component is believed to originate in the geometrically thin and optically thick Shakura-Sunyaev accretion disc (Shakura & Sunyaev 1973). One of the most plausible processes of formation of the hard spectral component is Comptonization of soft disc photons on hot electrons (Sunyaev & Truemper 1979; Sunyaev & Titarchuk 1980). The Comptonization site is often referred to as a corona. Although it is generally accepted that the Comptonizing corona has to be located in the close vicinity of the black hole, there are currently different ideas brought up on the detailed geometry of the region. The overall behaviour of the SF-QPO and  $\Gamma$ -QPO relations can be explained qualitatively within the “sombbrero” geometry (Poutanen et al. 1997; Gilfanov 2010). In this configuration, a quasi-spherical corona surrounds the black hole and the accretion disc extends a short distance into the corona. In the LHS the disc is truncated at a large radius and the remaining space is filled by the hot, optically thin corona (Done et al. 2007; Gierliński et al. 2008; D’Angelo et al. 2008; Tomsick et al. 2009; Hiemstra et al. 2009). While during the HSS, the disc reaches the inner most stable orbit leaving (at most) only little space for the corona. A fraction of the Comptonized photons emitted from the corona irradiates the accretion disc. Some of them are reflected due to Compton Scattering (Basko et al. 1974). We note that there are claims that the disc reaches the inner most stable orbit even in the LHS (Miller et al. 2006a,b; Rykoff et al. 2007). There are also models which predict a hot inner and a cool outer disc separated by a gap filled with an advection-dominated accretion flow (Liu et al. 2007).

Coming back to the sombrero geometry, which matches our findings, the QPOs correspond to oscillations in a transition layer between the disc and the hotter Comptonizing region (Nobili et al.

2000; Ingram et al. 2009; Ingram & Done 2011). The QPO frequency is inversely related to the truncation radius of the disc, as it is in most models (see e.g. Titarchuk & Osherovich 2000; Chakrabarti & Manickam 2000). While the system evolves from the LHS to the HIMS the truncation radius moves inward and the QPO frequency increases. In the sombrero configuration the solid angle of the disc seen by the hot electrons correlate with the fraction of disc emission reaching the corona. As the disc expands towards the black hole, the reflection scaling factor increases, the fraction of up-scattered photons decreases and the spectrum steepens (Zdziarski et al. 1999; Gilfanov 2010). Thus the observed (anti-)correlations between QPO frequency and spectral parameters can be explained within the sombrero geometry.

## 5 CONCLUSION

We studied correlations between spectral and timing parameters for observations with type-C QPOs. The sample comprised observations of GX 339-4, H 1743-322, and XTE J1650-500. Our investigations confirmed the known positive correlation between photon index and centroid frequency of the QPOs and revealed an anti-correlation between the fraction of up-scattered photons and the QPO frequency. We showed that both correlations behaved as expected in the “sombbrero” geometry, which also predicted the observed correlation between photon index and reflection scaling factor (Gilfanov 2010). Furthermore, we showed that during outburst decay the correlation between photon index and QPO frequency followed a general track, independent of individual outbursts.

## ACKNOWLEDGMENTS

The research leading to these results has received funding from the European Community’s Seventh Framework Programme (FP7/2007-2013) under grant agreement number ITN 215212 “Black Hole Universe”. SM and TB acknowledge support from grant ASI-INAF I/009/10/0. This work makes use of EURO-VO software, tools or services. The EURO-VO has been funded by the European Commission through contracts RI031675 (DCA) and 011892 (VO-TECH) under the 6th Framework Programme and

contracts 212104 (AIDA) and 261541 (VO-ICE) under the 7th Framework Programme.

## References

- Arnaud K. A., 1996, in G. H. Jacoby & J. Barnes ed., *Astronomical Data Analysis Software and Systems V* Vol. 101 of *Astronomical Society of the Pacific Conference Series*, XSPEC: The First Ten Years. p. 17
- Basko M. M., Sunyaev R. A., Titarchuk L. G., 1974, *A&A*, 31, 249
- Belloni T., Hasinger G., 1990, *A&A*, 227, L33
- Belloni T., Homan J., Casella P., van der Klis M., Nespoli E., Lewin W. H. G., Miller J. M., Méndez M., 2005, *A&A*, 440, 207
- Belloni T., Parolin I., Del Santo M., Homan J., Casella P., Fender R. P., Lewin W. H. G., Méndez M., Miller J. M., van der Klis M., 2006, *MNRAS*, 367, 1113
- Belloni T., Psaltis D., van der Klis M., 2002, *ApJ*, 572, 392
- Belloni T. M., 2010, in T. Belloni ed., *Lecture Notes in Physics*, Berlin Springer Verlag Vol. 794 of *Lecture Notes in Physics*, Berlin Springer Verlag, *States and Transitions in Black Hole Binaries*. pp 53
- Belloni T. M., Motta S. E., Muñoz-Darias T., 2011, *Bulletin of the Astronomical Society of India*, 39, 409
- Capitanio F., Belloni T., Del Santo M., Ubertini P., 2009, *MNRAS*, 398, 1194
- Casella P., Belloni T., Stella L., 2005, *ApJ*, 629, 403
- Chakrabarti S. K., Manickam S. G., 2000, *ApJ*, 531, L41
- D'Angelo C., Giannios D., Dullemond C., Spruit H., 2008, *A&A*, 488, 441
- Di Matteo T., Psaltis D., 1999, *ApJ*, 526, L101
- Done C., Gierliński M., Kubota A., 2007, *A&ARv*, 15, 1
- Fender R. P., Homan J., Belloni T. M., 2009, *MNRAS*, 396, 1370
- Garcia M. R., McClintock J. E., Narayan R., Callanan P. J., 1998, in S. Howell, E. Kuulkers, & C. Woodward ed., *Wild Stars in the Old West* Vol. 137 of *Astronomical Society of the Pacific Conference Series*, *Black Hole Event Horizons and X-ray Nova Luminosities - Update*. pp 506
- Gierliński M., Done C., Page K., 2008, *MNRAS*, 388, 753
- Gierliński M., Newton J., 2006, *MNRAS*, 370, 837
- Gilfanov M., 2010, in T. Belloni ed., *Lecture Notes in Physics*, Berlin Springer Verlag Vol. 794 of *Lecture Notes in Physics*, Berlin Springer Verlag, *X-Ray Emission from Black-Hole Binaries*. pp 17
- Gou L., McClintock J. E., Reid M. J., Orosz J. A., Steiner J. F., Narayan R., Xiang J., Remillard R. A., Arnaud K. A., Davis S. W., 2011, *ApJ*, 742, 85
- Hiemstra B., Soleri P., Méndez M., Belloni T., Mostafa R., Wijnands R., 2009, *MNRAS*, 394, 2080
- Homan J., Belloni T., 2005, *Ap&SS*, 300, 107
- Homan J., Wijnands R., van der Klis M., Belloni T., van Paradijs J., Klein-Wolt M., Fender R., Méndez M., 2001, *ApJS*, 132, 377
- Houck J. C., Denicola L. A., 2000, in N. Manset, C. Veillet, & D. Crabtree ed., *Astronomical Data Analysis Software and Systems IX* Vol. 216 of *Astronomical Society of the Pacific Conference Series*, *ISIS: An Interactive Spectral Interpretation System for High Resolution X-Ray Spectroscopy*. pp 591
- Ingram A., Done C., 2011, *MNRAS*, 415, 2323
- Ingram A., Done C., Fragile P. C., 2009, *MNRAS*, 397, L101
- Kalemci E., 2002, PhD thesis, UNIVERSITY OF CALIFORNIA, SAN DIEGO
- Kalemci E., Tomsick J. A., Rothschild R. E., Pottschmidt K., Corbel S., Wijnands R., Miller J. M., Kaaret P., 2003, *ApJ*, 586, 419
- Leahy D. A., Elsner R. F., Weisskopf M. C., 1983, *ApJ*, 272, 256
- Liu B. F., Taam R. E., Meyer-Hofmeister E., Meyer F., 2007, *ApJ*, 671, 695
- Magdziarz P., Zdziarski A. A., 1995, *MNRAS*, 273, 837
- McClintock J. E., Remillard R. A., 2006, *Black hole binaries*. pp 157–213
- McClintock J. E., Remillard R. A., Rupen M. P., Torres M. A. P., Steeghs D., Levine A. M., Orosz J. A., 2009, *ApJ*, 698, 1398
- Merloni A., Fabian A. C., Ross R. R., 2000, *MNRAS*, 313, 193
- Miller J. M., Homan J., Miniutti G., 2006a, *ApJ*, 652, L113
- Miller J. M., Homan J., Steeghs D., Rupen M., Hunstead R. W., Wijnands R., Charles P. A., Fabian A. C., 2006b, *ApJ*, 653, 525
- Mitsuda K., Inoue H., Koyama K., Makishima K., Matsuoka M., Ogawara Y., Suzuki K., Tanaka Y., Shibazaki N., Hirano T., 1984, *PASJ*, 36, 741
- Motta S., Muñoz-Darias T., Belloni T., 2010, *MNRAS*, 408, 1796
- Motta S., Muñoz-Darias T., Casella P., Belloni T., Homan J., 2011, *MNRAS*, 418, 2292
- Muñoz-Darias T., Motta S., Belloni T. M., 2011, *MNRAS*, 410, 679
- Nobili L., Turolla R., Zampieri L., Belloni T., 2000, *ApJ*, 538, L137
- Nowak M. A., Wilms J., Heinz S., Pooley G., Pottschmidt K., Corbel S., 2005, *ApJ*, 626, 1006
- Poutanen J., Krolik J. H., Ryde F., 1997, *MNRAS*, 292, L21
- Remillard R. A., McClintock J. E., 2006, *Annual Rev. of A&A*, 44, 49
- Remillard R. A., Muno M. P., McClintock J. E., Orosz J. A., 2002a, *ApJ*, 580, 1030
- Remillard R. A., Sobczak G. J., Muno M. P., McClintock J. E., 2002b, *ApJ*, 564, 962
- Rykoff E. S., Miller J. M., Steeghs D., Torres M. A. P., 2007, *ApJ*, 666, 1129
- Shakura N. I., Sunyaev R. A., 1973, *A&A*, 24, 337
- Shaposhnikov N., Titarchuk L., 2009, *ApJ*, 699, 453
- Steiner J. F., Narayan R., McClintock J. E., Ebisawa K., 2009, *PASP*, 121, 1279
- Stiele H., Motta S., Muñoz-Darias T., Belloni T. M., 2011, *MNRAS*, 418, 1746
- Stiele H., Muñoz-Darias T., Motta S., Belloni T. M., 2012, *MNRAS*, 422, 679
- Sunyaev R. A., Titarchuk L. G., 1980, *A&A*, 86, 121
- Sunyaev R. A., Truemper J., 1979, *Nature*, 279, 506
- Tamura M., Kubota A., Yamada S., Done C., Kolehmainen M., Ueda Y., Torii S., 2012, *ApJ*, 753, 65
- Titarchuk L., Mastichiadis A., Kylafis N. D., 1997, *ApJ*, 487, 834
- Titarchuk L., Osheroich V., 2000, *ApJ*, 542, L111
- Tomsick J. A., Kalemci E., Kaaret P., 2004, *ApJ*, 601, 439
- Tomsick J. A., Yamaoka K., Corbel S., Kaaret P., Kalemci E., Migliari S., 2009, *ApJ*, 707, L87
- Vignarca F., Migliari S., Belloni T., Psaltis D., van der Klis M., 2003, *A&A*, 397, 729
- Wijnands R., Homan J., van der Klis M., 1999, *ApJ*, 526, L33
- Wilms J., Allen A., McCray R., 2000, *ApJ*, 542, 914
- Zdziarski A. A., Gierliński M., Mikołajewska J., Wardziński G., Smith D. M., Harmon B. A., Kitamoto S., 2004, *MNRAS*, 351, 791

Zdziarski A. A., Lubinski P., Smith D. A., 1999, MNRAS, 303,

L11

Zhang W., Jahoda K., Swank J. H., Morgan E. H., Giles A. B.,  
1995, ApJ, 449, 930

This paper has been typeset from a  $\text{\TeX}$ / $\text{\LaTeX}$  file prepared by the author.